

A Unified Approach for Numerical Simulation of Viscous
Compressible and Incompressible Flows over
Adiabatic and Isothermal Walls
M.Hafez, M.Soliman
University of California, Davis
and
S.White
NASA Ames Research Center

S31-34
16049/p-18

Abstract

A new formulation (including the choice of variables, their non-dimensionalization and the form of the artificial viscosity) is proposed for the numerical solution of the full Navier-Stokes equations for compressible and incompressible flows with heat transfer.

With the present approach, the same code can be used for constant as well as variable density flows. The changes of the density due to pressure and temperature variations are identified and it is shown that the low Mach number approximation is a special case. At zero Mach number, the density changes due to the temperature variation is accounted for, mainly through a body force term in the momentum equation. It is also shown that the Boussinesq approximation of the buoyancy effects in an incompressible flow is a special case.

To demonstrate the new capability, three examples are tested. Flows in driven cavities with adiabatic and isothermal walls are simulated with the same code as well as incompressible and supersonic flows over a wall with and without a groove. Finally, viscous flow simulations of an oblique shock reflection from a flat plate are shown to be in good agreement with the solutions available in literature.

Introduction

In a previous work[1], the authors proposed a formulation for both compressible and incompressible viscous flow simulation. First the density is eliminated in terms of the pressure and the temperature via the perfect gas equation of state. This step by itself is not sufficient simply because the equation of state is not valid for incompressible flows. The formulation is completed using the

perturbation of the pressure and the temperature relative to reference values as the dependant variables. It is shown that the density in terms of these new variables approaches a constant as the reference Mach number vanishes. The above formulation is generalized in the present paper to allow for incompressible flows which are not necessarily isothermal.

To obtain a numerical solution, an artificial dissipation is introduced by adding to the governing equations the Laplacians of the pressure and the velocity components. An improved model is also tested which is based on a partial least square procedures. The continuity equation is modified by a Poission's equation for the pressure similar to that of Harlow and Welch[2], and Harlow and Amsden[3]. The momentum equations are also modified by Poission's equations of the velocity components. The first modification is obtained by taking the divergence of the momentum equations, while the second modification can be related to a vector identity relating the Laplacian of the velocity vector to the gradient of its divergence and the curl of the vorticity. In both modifications, the evaluation of the nonhomogeneous terms of the Poissions equations are lagged as in the deferred correction procedures.

The energy equation is augmented with second order terms of the total enthalpy obtained via minimizing the squares of the convective terms. This modification is very small in the neighborhood of a solid surface and can be interpreted as an artificial streamline diffusion as in the work of Hughes etal[4].

The present numerical solutions are obtained using a standard Glarkin procedure. The resulting nonlinear system of equations are solved via Newton's method. At each iteration a direct solver based on banded Gaussion elimination is

employed. The use of finite element discretizations and direct solvers are not necessary to obtain numerical solutions based on the present formulations, and other viable alternatives are, for example, finite volumes and iterative procedures.

In the following, the derivation of the governing equations and the applications to some test problems are discussed.

Governing Equations

For steady compressible viscous flows, the continuity, momentum and energy equations can be written in terms of the primitive variables (ρ, p, \vec{q}) including the effects of a body force as :

$$\begin{aligned} \nabla \cdot \rho \vec{q} &= 0 \\ \nabla \cdot \rho \vec{q} \vec{q} &= \nabla : \tau + \rho \vec{f} \\ \nabla \cdot \rho \vec{q} H &= \nabla \cdot k \nabla T + \nabla \cdot (\tau \cdot \vec{q}) + \rho \vec{f} \cdot \vec{q} \end{aligned} \quad (1)$$

where $H = \frac{\gamma p}{\gamma - 1 \rho} + \frac{1}{2} (u^2 + v^2)$

and $\tau_{ij} = \lambda (\nabla \cdot \vec{q}) \delta_{ij} + \mu \left(\frac{\partial q_i}{\partial x_j} + \frac{\partial q_j}{\partial x_i} \right)$

For convenience it is assumed that $\lambda = -\frac{2}{3}\mu$ and $p = \rho R T$. The two constants R and γ are related to the specific heat constants c_p and c_v ; $R = c_p - c_v$ and $\gamma = \frac{c_p}{c_v}$. For the derivation of the above equations, see, for example, Liepman and Roshko [5]

A standard non-dimensional form is obtained using the reference values of ρ and q in the far field of external flow problems. The pressure is usually normalized by $\rho_\infty q_\infty^2$ and the temperature by q_∞^2 / c_p . If L is a characteristic length, two parameters appear in the equations namely the Reynolds and Peclet numbers, where

$$Re = \frac{\rho_\infty q_\infty L}{\mu_\infty} \quad (2)$$

$$Pe = \frac{\rho_\infty q_\infty L}{k_\infty / c_p} \quad (3)$$

The Peclet number is the product of Prandtl and Reynolds numbers, where

$$Pr = \frac{\mu_\infty}{k_\infty / c_p} \quad (4)$$

Equations (1) becomes

$$\begin{aligned} \nabla \cdot \rho \vec{q} &= 0 \\ \nabla \cdot \rho \vec{q} \vec{q} &= -\nabla p + \frac{1}{Re} \nabla : \tau - \frac{1}{Fr} \rho K \\ \nabla \cdot \rho \vec{q} H &= \frac{1}{Pe} \nabla \cdot k \nabla T + \frac{1}{Re} \nabla \cdot (\tau \cdot \vec{q}) - \frac{1}{Fr} \vec{q} \cdot \rho K \end{aligned} \quad (5)$$

In equations (5), the relative effect of gravity is identified by the Froude number,

$$Fr = \frac{q_\infty^2}{g L} \quad (6)$$

In natural convection problems, the variation of density due to temperature difference ΔT creates a buoyancy term in the momentum equation. To first order accuracy, the density variation would be $\rho = \rho_\infty (1 - \beta \Delta T)$ where β is the thermal expansion coefficient, hence the buoyancy term is given by

$$\frac{\beta \Delta T}{2} \frac{g L}{q_\infty} \frac{\vec{q}}{K} = \frac{Gr}{2} \frac{\vec{q}}{K} \quad (7)$$

where

$$Gr = \frac{\beta \Delta T g L^3}{\mu_\infty} \quad (8)$$

The above formulation is not suitable for incompressible flows since in the limit of zero free stream Mach number, both the normalized pressure and temperature are unbounded. Two new variables were introduced in the previous study to avoid

this problem, namely p^* and T^* where

$$p^* = p - p_\infty = p - \frac{1}{\gamma M_\infty^2} \quad (9)$$

and,

$$\bar{T}^* = \bar{T} - \bar{T}_\infty = \bar{T} - \frac{1}{(\gamma-1) M_\infty^2} \quad (10)$$

Hence, the equation of state gives

$$\bar{\rho} = \frac{\gamma M_\infty^2 p^* + 1}{(\gamma-1) M_\infty^2 T^* + 1} \quad (11)$$

As the Mach number vanishes, the normalized density $\bar{\rho}$ approaches 1.0, i.e. the reduced incompressible flow is isothermal. To allow for density variations due to temperature changes in the incompressible limit, in cases of adiabatic walls as well as walls with specified temperatures, the variable T^* is replaced by

$$\bar{T} = \frac{T}{T_\infty} \quad (12)$$

Equation (11) becomes

$$\bar{\rho} = \frac{\gamma M_\infty^2 p^* + 1}{\bar{T}} \quad (13)$$

In the limit of zero Mach number, $\bar{\rho} \bar{T}$ approaches 1 and the proper general dependence of the density on the temperature is recovered. The isothermal flow is of course a special case of the above relation.

The continuity and the momentum equations are unaltered, the energy equation becomes

$$\bar{\nabla} \cdot \bar{\rho} \bar{q} \bar{H} = \frac{1}{Pe} \bar{\nabla} \cdot k \bar{\nabla} \bar{T} + \frac{Ec_w}{Re} \bar{\nabla} \cdot (\bar{\tau} \cdot \bar{q}) - \frac{Ec_w}{Fr} \bar{q} \cdot \bar{\rho} \bar{K} \quad (14)$$

where

$$\bar{H} = \bar{T} + Ec_w q^2 / 2$$

and,

$$Ec = \frac{q_\infty^2}{c_p T_\infty} = (\gamma-1) M_\infty^2 \quad (Ec \text{ is the Eckert number})$$

The incompressible limit of Equation (14) is

$$\bar{\nabla} \cdot \bar{\rho} \bar{q} \bar{T} = \frac{1}{Pe} \bar{\nabla} \cdot k \bar{\nabla} \bar{T} \quad (15)$$

Here, the temperature ratio T_w/T_∞ , where T_w is the average wall specified temperature, enters only through the boundary conditions.

Alternatively, one can choose

$$\bar{T} = \frac{T}{T_\infty} \frac{T_\infty}{T_w} = \bar{T} \frac{T_\infty}{T_w} \quad (12)$$

and, in this case

$$\bar{\rho} = \frac{\gamma M_\infty^2 p^* + 1}{\bar{T} \frac{T_w}{T_\infty}} \quad (13)$$

and

$$\bar{\nabla} \cdot \bar{\rho} \bar{q} \bar{H} = \frac{1}{Pe} \bar{\nabla} \cdot k \bar{\nabla} \bar{T} + \frac{Ec_w}{Re} \bar{\nabla} \cdot (\bar{\tau} \cdot \bar{q}) - \frac{Ec_w}{Fr} \bar{q} \cdot \bar{\rho} \bar{K} \quad (14)$$

where

$$\bar{H} = \bar{T} + Ec_w q^2 / 2$$

and

$$Ec_w = \frac{q_\infty^2}{c_p T_w} = \frac{(\gamma-1) M_\infty^2}{T_w/T_\infty}$$

Thus, the present formulation is valid for compressible and incompressible flows, with adiabatic or specified temperature walls. Moreover, it is clear from equation

(13) or (13) that the low Mach number approximation (see for example Rhem and Baum [6], Majda[7] and Markle[8]) is a special case. The Boussinesq approximation of the buoyancy effects in an incompressible flow is also a special case of the present formulation.

It should be mentioned that the above formulation is not restricted to perfect gases. A more general equation of state can be written in the form

$$\rho = \rho_\infty + \frac{\partial \rho}{\partial T} \Delta T + \frac{\partial \rho}{\partial p} \Delta p \quad (16)$$

or in the non-dimensional form

$$\bar{p} = 1 + \frac{\partial \bar{p}}{\partial \bar{T}} \Delta \bar{T} + \frac{\partial \bar{p}}{\partial \bar{p}^*} \Delta \bar{p}^* \quad (16)$$

The last term of equation (16) always vanishes in the limit of zero Mach number.

Numerical Method

It is well known that centered schemes permit, in general, odd and even decoupling of the discrete pressure field [9]. To avoid this problem, different interpolations are used for the velocity and the pressure in the standard finite element analysis of incompressible flows [10], [11]. Recently, Pironeau [12] addressed this issue for compressible flows as well.

It is also well known that centered schemes produce oscillatory solutions of convection-diffusion equations with high Reynolds numbers, unless impractical excessively fine meshes are used.

In the present study, artificial dissipation is introduced explicitly in all equations, to eliminate the wiggles and to allow for capturing shocks and contact discontinuities. Two forms of artificial viscosity are considered. In the first method, the governing equations become

$$\begin{aligned} \nabla \cdot \rho \vec{q} &= \epsilon_1 \nabla^2 p^* \\ \nabla \cdot \rho \vec{q} \vec{q} + \nabla p &= \frac{1}{Re} \nabla \cdot \tau + \frac{1}{Fr} \rho K = \epsilon_2 \nabla^2 \vec{q} \\ \nabla \cdot \rho \vec{q} H &= \frac{1}{Pe} \nabla \cdot k \nabla T + \frac{Ec}{Re} \nabla \cdot (\tau \cdot \vec{q}) + \frac{Ec}{Fr} \rho f \cdot \vec{g} = \epsilon_3 \nabla^2 H \end{aligned} \quad (17)$$

where ϵ 's are small parameters of the order of the mesh size. A standard Galerkin finite element method is applied to calculate the solution of equations (17). This form has been investigated before for both incompressible and compressible flows with the standard separate formulations. With the present unified approach, the same code is used to calculate compressible and incompressible cases.

In the second method, the Laplacian terms are balanced with nonlinear terms obtained by manipulating the original

equations. For example, the momentum equations can be written in the form

$$\nabla p = \vec{g} \quad (18)$$

A Poisson's equation is constructed by taking the divergence of equation (18) and allowing a variable (positive) artificial viscosity coefficient, one arrives at

$$\nabla \cdot \epsilon \nabla p = \nabla \cdot \epsilon \vec{g} \quad (18)$$

Equation (18) can be also obtained from minimizing the functional $\int \epsilon (\nabla p - \vec{g}) \cdot (\nabla p - \vec{g})$ with respect to p , assuming \vec{g} is known. The continuity equation is then modified by the Poisson's equation

(18).

Similarly, the Laplacian of the velocity components can be balanced using the vector identity

$$\nabla^2 \vec{q} = \nabla S - \nabla X \omega \quad (19)$$

where

$$S = \nabla \cdot \vec{q}$$

$$\omega = \nabla X \vec{q}$$

To allow for a variable viscosity coefficients, one can minimize the

functional (assuming S and ω known)

$$\int \epsilon (\nabla \cdot \vec{q} - S)^2 + \epsilon (\nabla X \vec{q} - \omega)^2$$

with respect to \vec{q} to obtain

$$\nabla \cdot \epsilon \nabla \vec{q} = \nabla \epsilon S - \nabla X \epsilon \omega + f(\nabla \epsilon) \quad (19)$$

In equations (18) and (19), the quantities \vec{g} , S and ω are obtained at each node from their definitions using a standard Galerkin finite element method with the same interpolation used for the other variables. The evaluation of these terms are lagged and their contributions to the Jacobians are neglected.

For the energy equation, the modification is obtained via minimizing

the functional $\int \epsilon (\rho \vec{q} \cdot \nabla H + \pi)^2$ with respect

to H . For convenience, π is dropped with the

justification that the artificial dissipation is mostly needed in the inviscid adiabatic part of the flow where the relatively coarse mesh is not capable of resolving the π term. In the neighborhood of a solid surface, a fine mesh is required anyway and there is no need there of artificial viscosity terms. The present modification is very small there since it is scaled with the velocity. The same remark is applicable for the treatment of the momentum equations where the viscous stress terms can be ignored in the evaluation of the g term.

The variational formulation of the artificial dissipation terms provides a natural treatment of the numerical boundary conditions. Upon integration by parts, the resulting line integrals are simply ignored.

Because the modification terms, for the continuity, the momentum and the energy equations are obtained separately by adopting a partial least squares procedure for each case the resulting algebraic system of equations are not necessarily symmetric. A full least squares procedure for all equations coupled together has been successfully used by the first author to introduce dissipative terms for the solution of Euler equations simulating transonic flows with sharp shock waves [13]. In this case, it is possible however to construct a symmetric positive definite system at each Newton's iteration by a proper choice of the coefficients of the artificial terms [Jiang & Povinelli [14]. Unfortunately, such choices result in smearing the discontinuities. For viscous flows, they write the Navier Stokes equations as a system of first order equations in terms of velocity, pressure and vorticity and then a full least squares procedure is applied. The resulting algebraic equations are symmetric positive definite, but the number of unknowns are increased (almost doubled for three dimensional problems).

Needless to say, more work is required to determine the optimal form of the modification terms and the associated solution procedures for the general flow case.

Numerical Results

Three test problems are solved using the present formulation. The first viscosity method is used for the first two problems. Since the Re is relatively low, no artificial viscosity in the momentum or the energy equation is needed ($\epsilon_2 = \epsilon_3 = 0$). For the modified continuity equation, a numerical boundary condition, $\frac{\partial p}{\partial n} = 0$ at the wall is enforced at the wall. The third problem is solved by the two viscosity methods. In the following some preliminary results are presented.

I. Driven Cavity with Adiabatic and Isothermal Walls

Incompressible ($M_\infty = 0$) and compressible flows ($M_\infty = 0.4$) are simulated for $Re = 100$ with adiabatic walls. The pressure contours of the converged solutions are plotted in figures (I-a) and (I-b) respectively. Next, the temperature at the upper and lower walls are fixed and the calculations are repeated. The pressure contours are plotted in figures (I-c) and (I-d) and the corresponding temperature contours are shown in figures (I-e) and (I-f).

The effects of compressibility and the difference of wall temperatures, are clearly depicted in these figures.

II- Incompressible and Supersonic Viscous Flows over a Wall with and Without a Groove

A uniform stream of $Re = 1000$ over a flat plate is simulated with the same code. The pressure and velocity profiles at different locations are plotted in figures (II-a) and (II-b) for the case of $M_\infty = 0$. For supersonic flow with $M_\infty = 3$, the pressure, velocity and temperature profiles are shown in figures (II-c), (II-d) and (II-e). The pressure, temperature and density contours are given in figures (II-f), (II-g) and (II-h). As expected, an oblique shock

wave is formed due to the boundary layer displacement effect.

Next, the calculations are repeated for a flat plate with a groove. The pressure profiles for the incompressible flow case is shown in figure (II-i), while the pressure, temperature and density contours of the supersonic case are plotted in figures (II-j), (II-k) and (II-l).

III- Inviscid and Viscous flow Simulations of Shock Reflection from a flat plate.

First, an inviscid supersonic flow ($M_\infty=2.0$) with a reflected shock is calculated. The results are in agreement with the exact solution. The pressure contours from the two artificial viscosity methods are plotted in figure (III-a) and (III-b). For a viscous supersonic flow at $Re=296000$ and $M_\infty=2.0$, the results are in agreement with those of MacCormack [15] and with experimental data. The velocity profiles before, within and after the separation bubble are plotted in figure (III-c). The skin friction distribution is shown in figure (III-d). The pressure contours from the first and second artificial viscosity methods are compared in figure (III-e) and (III-f).

Cartesian grids and bilinear elements are used for all the problems tested in this paper. Applications to transonic flows over airfoils using unstructured finite elements are reported in a separate paper [16].

Conclusions

A unified approach for a general flow simulation is presented. It is shown that all the normalized variables used in the formulation are always bounded and the proper variation of the density due to changes in pressure and temperature is recovered in the limit of zero Mach number.

Two artificial viscosity methods are applied to obtain numerical results for some test cases. The governing equations are modified by either Laplacian's or Poisson's equations for the pressure, the velocity components and the total enthalpy. Acceptable solutions are

obtained via a standard Galerkin finite element procedure, using equal order interpolations for all normalized variables.

The unified approach offers a convenient formulation which allows, using the same code, the simulation of compressible and incompressible flows where the walls are adiabatic, with specified temperature distributions or of mixed type. In particular, the low Mach number approximation as well as the Boussinesq approximation (of the buoyancy effects) are special cases of the present formulations.

Obviously, it is always possible to have more efficient flow simulations for some special cases. For example, when the speed of sound is finite, explicit schemes can be used to integrate the time dependent gas equations, in contrast to the incompressible flow case where a Poisson's equation of the pressure has to be solved, at each time step, to guarantee the conservation of mass during the time evolution process. Another example is the special case of incompressible (constant density) flow where the energy (temperature) equation decouples and the solution of the continuity and the momentum equations provide the pressure and the velocity components. Therefore, the use of the present unified approach for the above two examples is more costly compared to the use of two separate codes tailored for the specifics of these two cases. It is still necessary however to have a general code for all speeds and all possible boundary conditions to handle the cases of mixed nature.

Acknowledgement

This work has been supported by NASA Ames Research Center.

References

- [1] Hafez, M. and Soliman, M., "Numerical Solution of the Incompressible Navier-Stokes Equations in Primitive Variables on Unstaggered Grids.", AIAA paper 91-1561. see also, Hafez, M. and Ahmed, J., "Vortex Breakdown Simulation, Part III-Compressibility Effects." in Fourth

- Symposium on Num. and Phys Aspects of Aerodynamics Flows". Long Beach, Ca. 1989.
- [2] Harlow, F. and Welsh, J. " Numerical Calculations of Time Dependant Viscous Incompressible Flow with Free Surface.", Phys. Fluids, vol.80, pp.2182-2189, 1965.
- [3] Harlow, F. and Amseden, A., " A Numerical Fluid Dynamics Calculation Method for All Flow Speeds.", J.of Comp. Phys. vol.8, pp.197-213, 1971.
- [4] Hughes, T. and Brooks, A., " A Multidimensional Upwind Scheme With no Crosswind Diffusion.", in ' Finite Element Methods for Convection Dominated Flows.', The American Society of Mechanical Engineers, 1979.
- [5] Liepman, H. and Roshko, A., " Elements of Gas Dynamics.", Wiley, 1957.
- [6] Rehm, R. and Baum, H., " The Equations of Motion for Thermally Driven Buoyant Flows.", J. Res. Nat. Bur. Stand, vol.83, pp.297-311, 1978.
- [7] Majda, A., " Equations for Low Mach Number Combustion.", Report # 112, Center for Pure Appl. Math., Nov. 1982.
- [8] Merkle, C. and Choi, Y.H., " Computation of Compressible Flows at Very Low Mach Numbers.", AIAA paper 86-0351.
- [9] Peyret, R. and Taylor, T., " Computational Methods for Fluid Flow.", Springer, 1984.
- [10] Zienkiewicz, O., Szmlter, J and Peraire, J. " Compressible and Incompressible Flow; An Algorithm for all Seasons.", Comp. Methods Appl. Mech. Eng., vol.78, pp.105-121, 1990.
- [11] Hughes, T. and Franca, L., " A New Finite Element Formulation for Computational Fluid Dynamics: VII The Stokes Problem with Various Well-Posed Boundary Conditions : Symmetric Formulations That Converge for All Velocity/Pressure Spaces.", Comp. Methods in Appl. Mech. and Eng., vol.65, pp.85-96. 1987.
- [12] Pironneau, O., Proceedings of a Workshops on " Algorithmic Trends in CFD.", Hampton, VA. 1991, to be published by Springer Verlag.
- [13] Hafez, M. and Fernandez, G., " Finite Element Simulation of Compressible Flows with Shocks.", AIAA paper 91-1551.
- [14] Jiang, B. and Povinelli, L. " Least Squares Finite Element Method for Fluid Dynamics.", NASA TM 102352-ICOMP 89-23.
- [15] MacCormack, R., " A Numerical Method for Solving the Equations of Compressible Viscous Flow.", AIAA J., vol.20, no.9, pp.1275-1281, 1982.
- [16] Baruzzi, G., Habashi, W. and Hafez, M., " An Improved Finite Element Method for the solution of the Compressible Navier-Stokes Equations", submitted to National Fluid Dynamics Congress, L.A, CA. 1992.

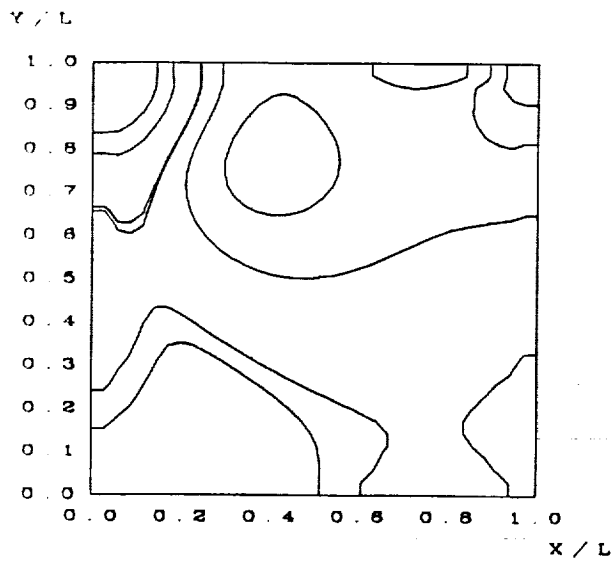


Fig.(I-a) Pressure contours
Incompressible Flow
Grid 36x36

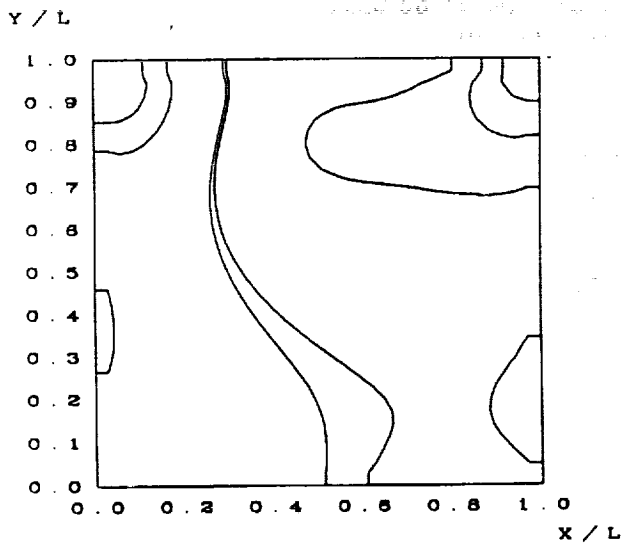


Fig.(I-b) Pressure Contours
Compressible Flow ($M_r=0.4$)
Grid 36x36

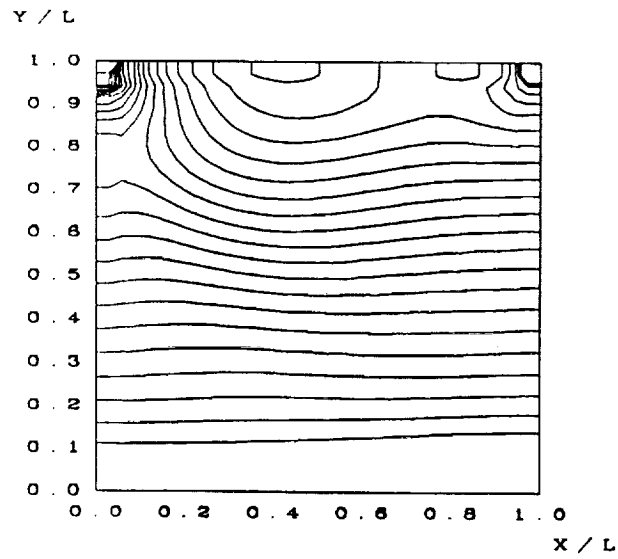


Fig.(I-c) Pressure Contours
Incompressible Flow
Grid 36x36
Upper Wall Temp.= 1.0
Lower Wall Temp.= 0.5

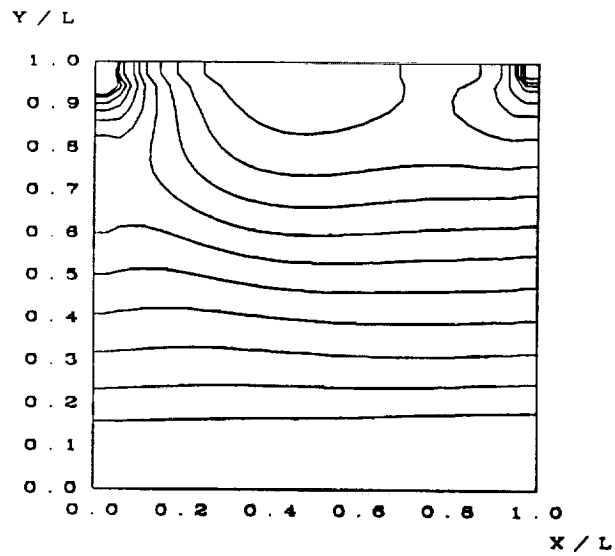


Fig.(I-d) Pressure Contours
Compressible Flow ($M_r=0.4$)
Grid 36x36
Upper Wall Temp.= 1.0
Lower Wall Temp.= 0.5

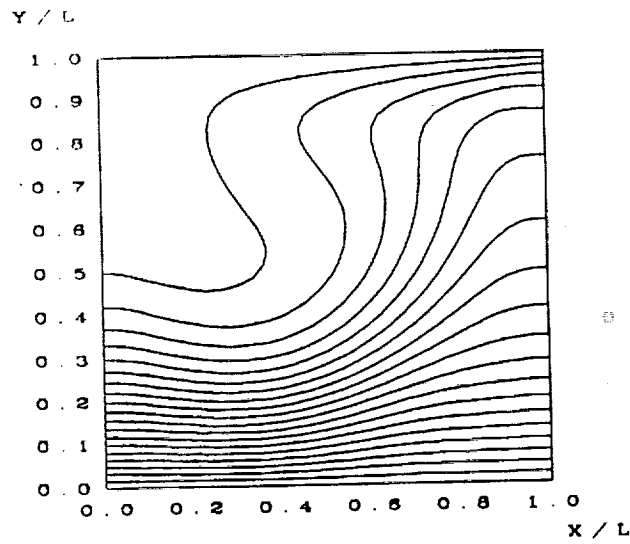


Fig.(I c) Temperature Contours
 Incompressible Flow
 Grid 36x36
 Upper Wall Temp.= 1.0
 Lower Wall Temp.= 0.5

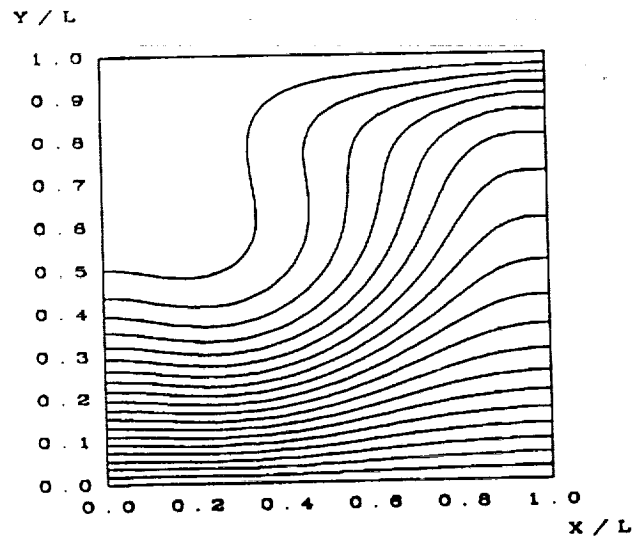


Fig.(I-f) Temperature Contours
 Compressible Flow ($M_r=0.4$)
 Grid 36x36
 Upper Wall Temp.= 1.0
 Lower Wall Temp.= 0.5

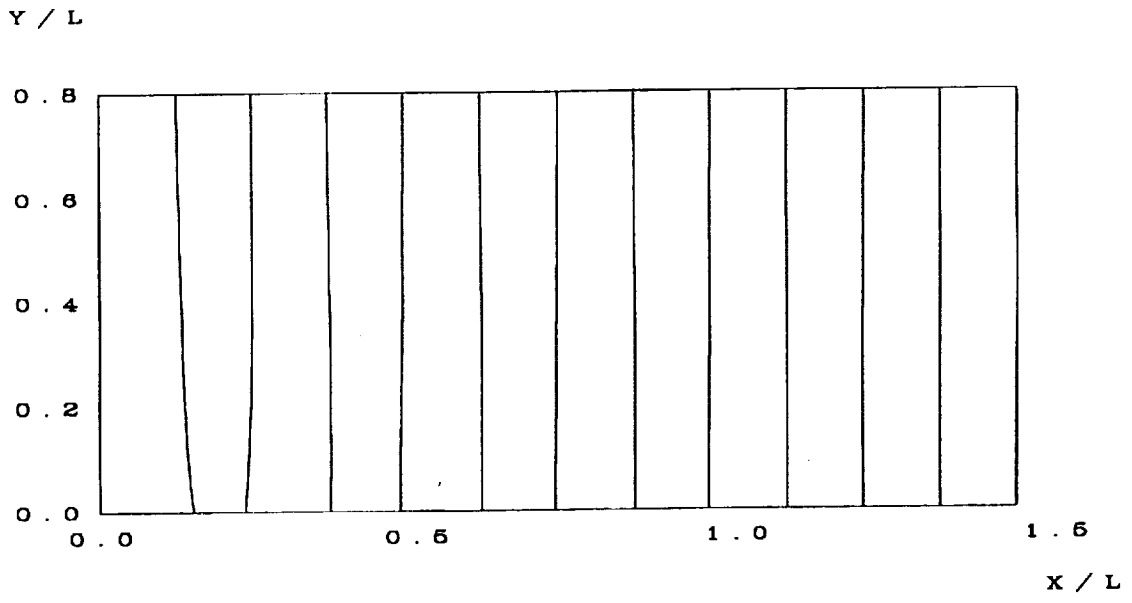


Fig.(II-a) Pressure Profiles
Incompressible Flow
Grid 26x31

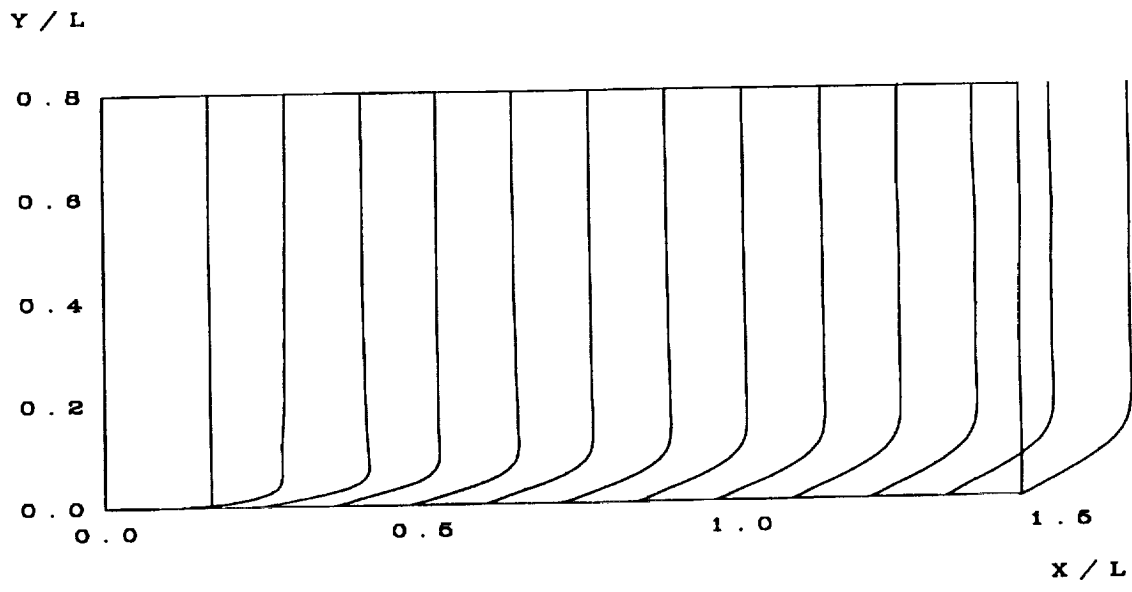


Fig.(II-b) Velocity Profiles
Incompressible Flow
Grid 26x31

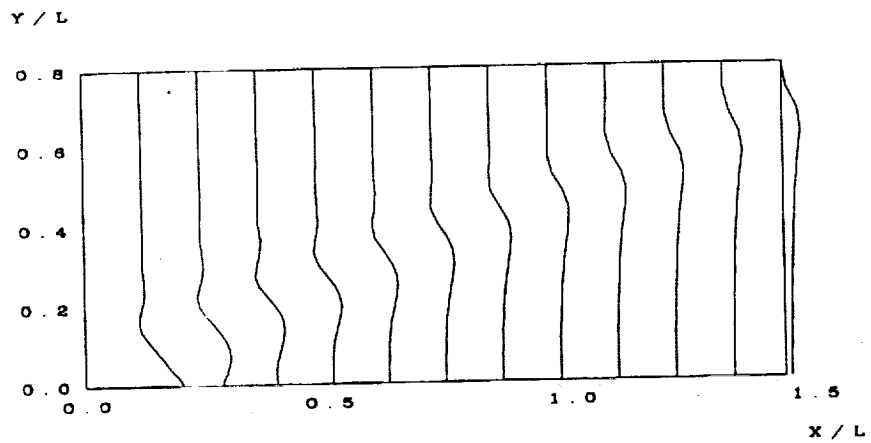


Fig.(II-c) Pressure Profiles
Supersonic Flow ($M_\infty=3$)
Grid 26x31

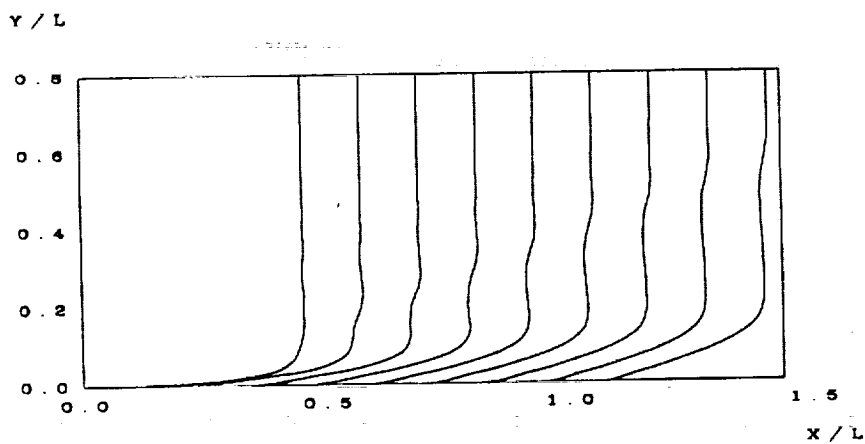


Fig.(II-d) Velocity Profiles
Supersonic Flow ($M_\infty=3$)
Grid 26x31

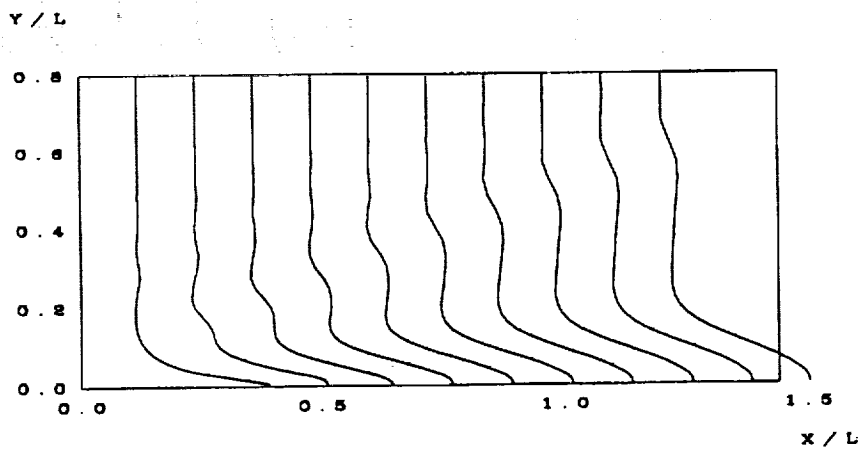


Fig.(II-e) Temperature Profiles
Supersonic Flow ($M_\infty=3$)
Grid 26x31

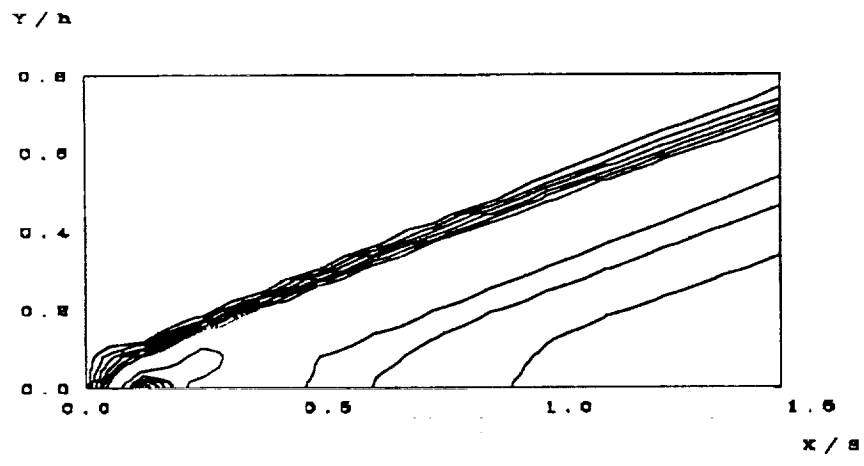


Fig.(II-f) Pressure Contours
Supersonic Flow ($M_\infty=3$)
Grid 26x31

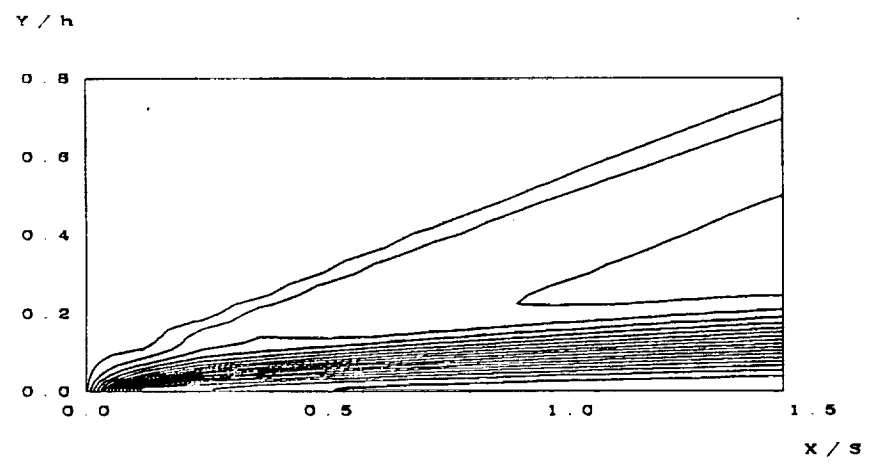


Fig.(II-g) Temperature Contours
Supersonic Flow ($M_\infty=3$)
Grid 26x31

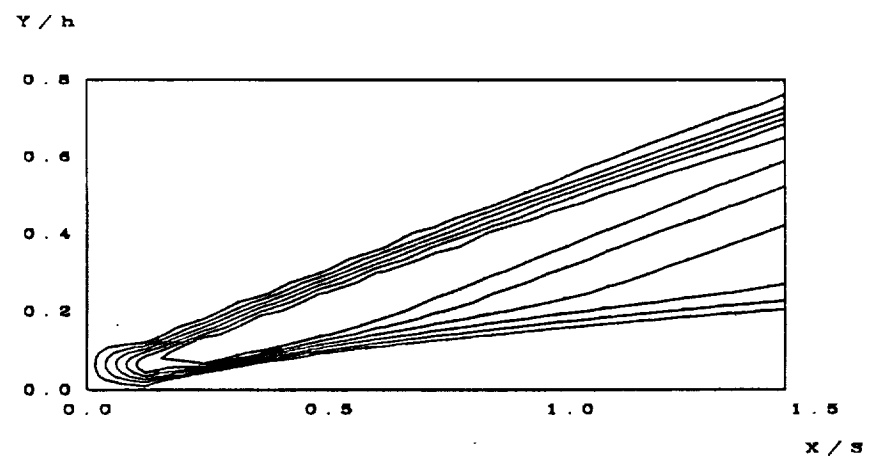


Fig.(II-h) Density Contours
Supersonic Flow ($M_\infty=3$)
Grid 26x31

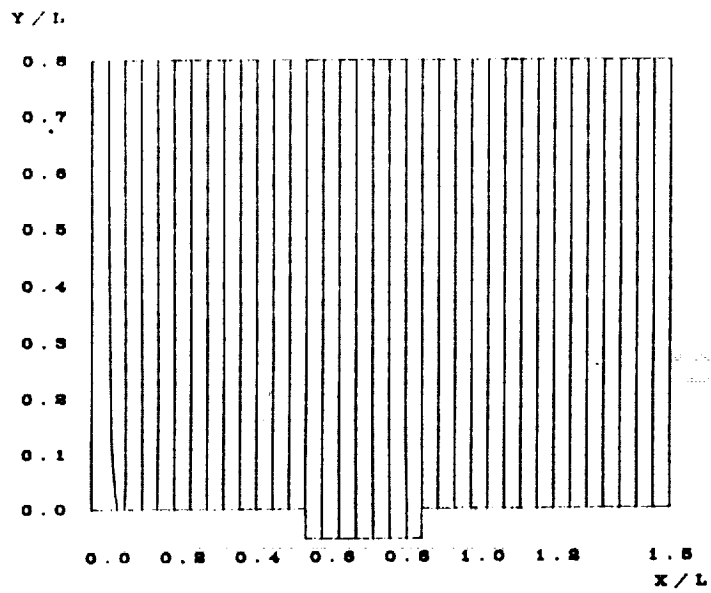


Fig.(II-i) Pressure Profiles
Supersonic Flow ($M_\infty = 3$)
Grid 36x38

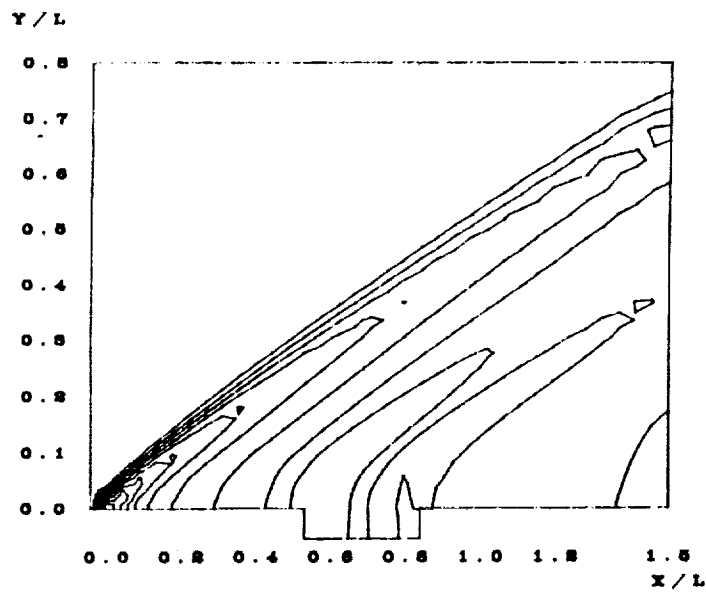


Fig.(II-j) Pressure Contours
Supersonic Flow ($M_\infty = 3$)
Grid 36x38

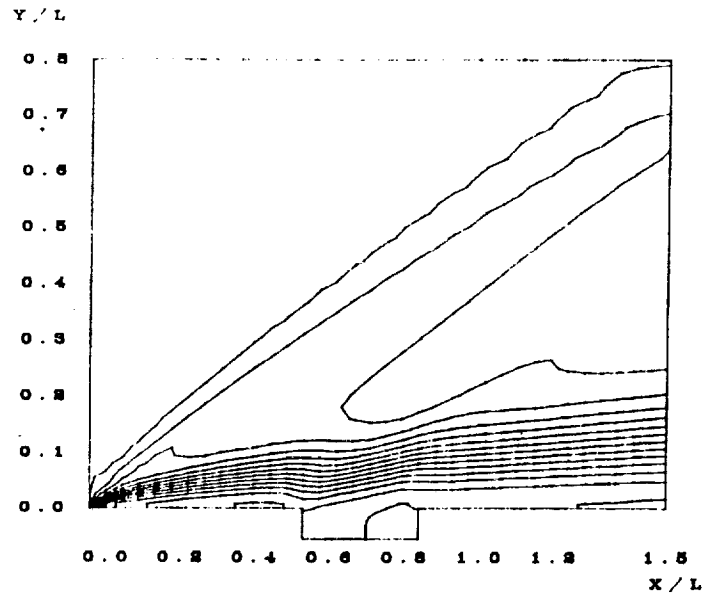


Fig.(II-k) Temperature Contours
Supersonic Flow ($M_{\infty}=3$)
Grid 36x38

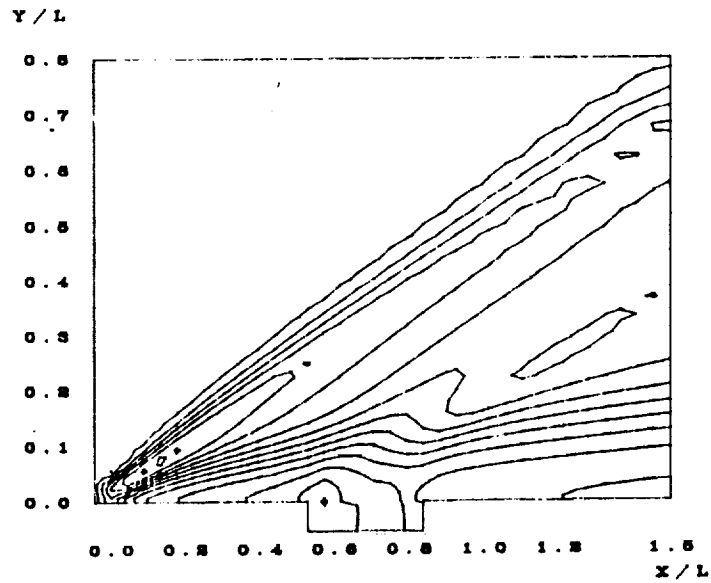
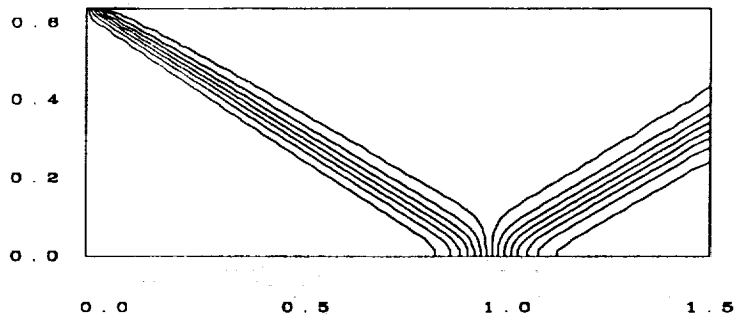


Fig.(II-l) Density Contours
Supersonic Flow ($M_{\infty}=3$)
Grid 36x38

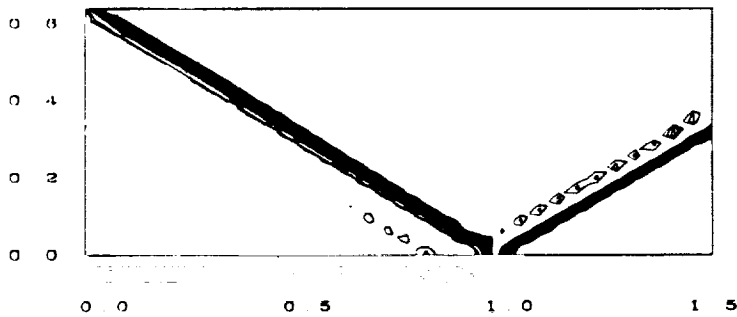
Y / h



x / S

Fig.(III-a) Pressure Contours
Inviscid Flow ($M_\infty=2$)
Grid 34x44
Viscosity Method #1

Y / L



x / L

Fig.(III-b) Pressure Contours
Inviscid Flow ($M_\infty=2$)
Grid 34x44
Viscosity Method #2

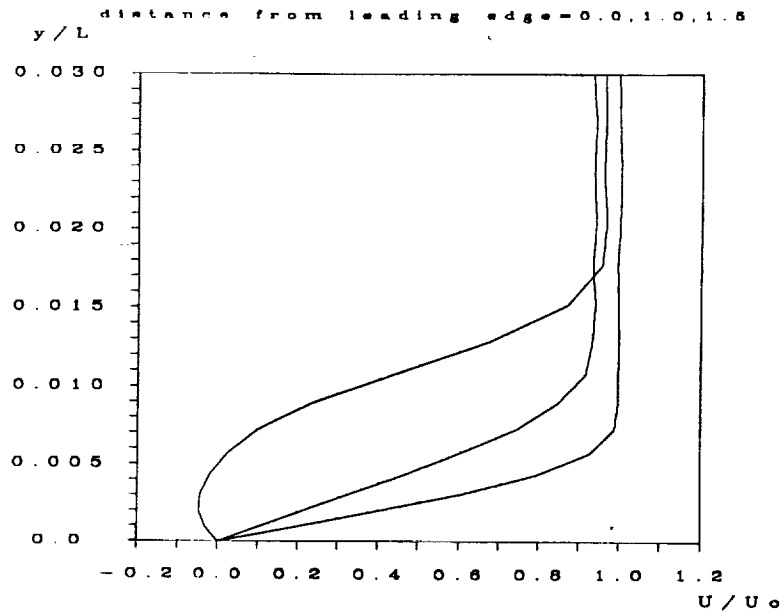


Fig.(III-c) Velocity Profiles
Viscous Flow ($M_\infty=2$)
Grid 34x44

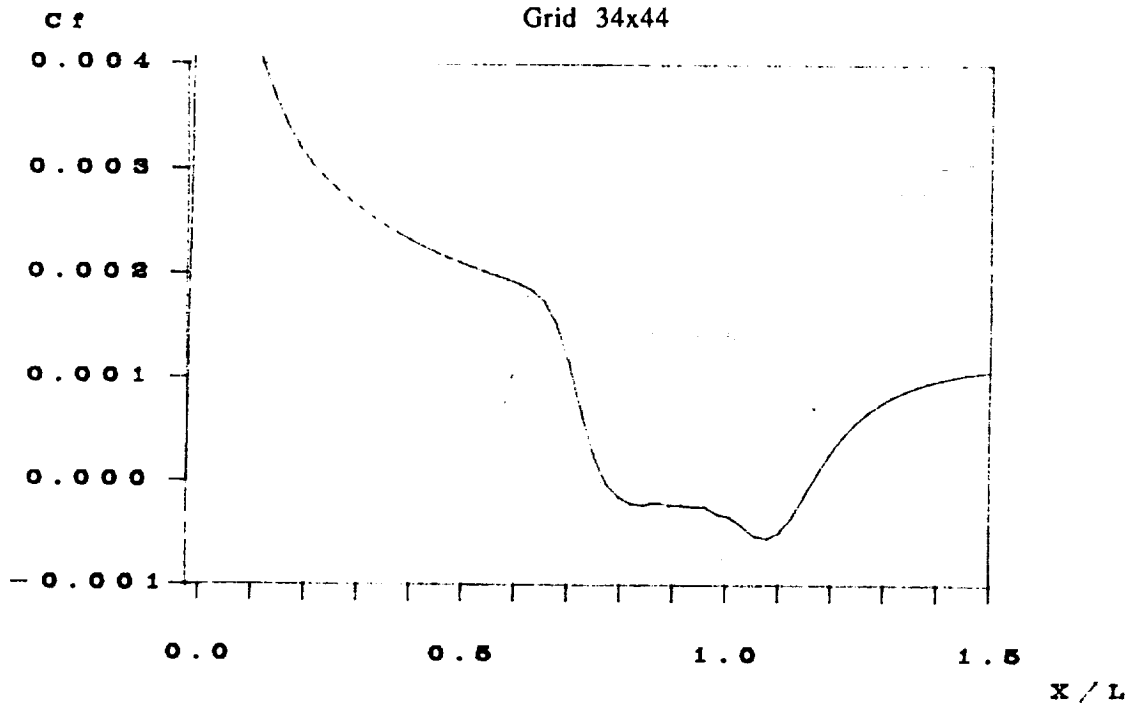
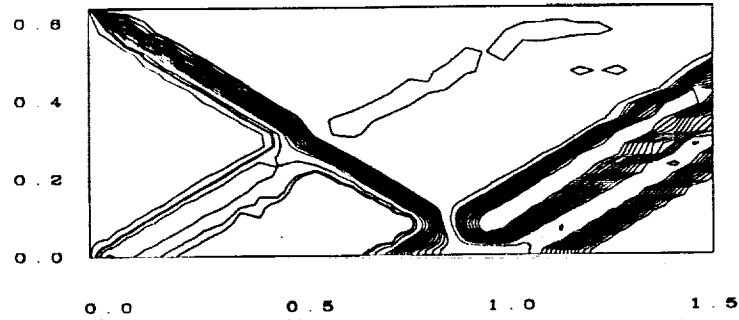


Fig.(III-d) Skin Friction Distribution
Viscous Flow ($M_\infty=2$)
Grid 56x44

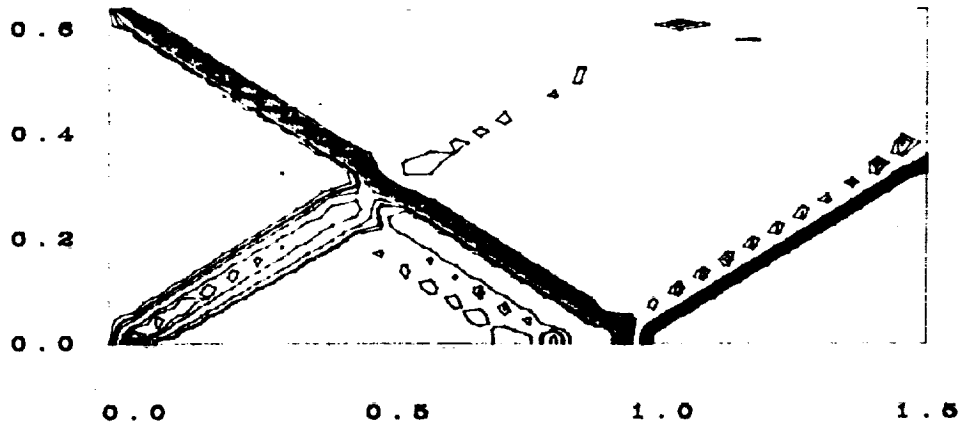
Y / L



X / L

Fig.(III-e) Pressure Contours
Viscous Flow ($M_\infty=2$)
Grid 34x44
Viscosity Method #1

Y / L



X / L

Fig.(III-f) Pressure Contours
Viscous Flow ($M_\infty=2$)
Grid 34x44
Viscosity Method #2